

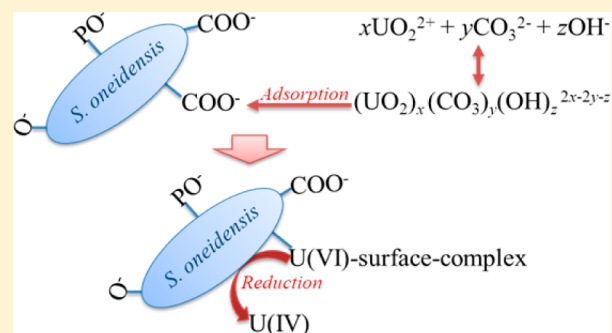
# Uranium Reduction by *Shewanella oneidensis* MR-1 as a Function of $\text{NaHCO}_3$ Concentration: Surface Complexation Control of Reduction Kinetics

Ling Sheng\* and Jeremy B. Fein

Department of Civil & Environmental Engineering & Earth Sciences, University of Notre Dame, Notre Dame, Indiana 46556, United States

## S Supporting Information

**ABSTRACT:** It is crucial to determine the controls on the kinetics of U(VI) bioreduction in order to understand and model the fate and mobility of U in groundwater systems and also to enhance the effectiveness of U bioremediation strategies. In this study, we measured the rate of U(VI) reduction by *Shewanella oneidensis* strain MR-1 as function of  $\text{NaHCO}_3$  concentration. The experiments demonstrate that increasing concentrations of  $\text{NaHCO}_3$  in the system lead to slower U(VI) reduction kinetics. The  $\text{NaHCO}_3$  concentration also strongly affects the speciation of U(VI) on the bacterial cell envelope. We used a thermodynamic surface complexation modeling approach to determine the speciation and concentration of U(VI) adsorbed onto the bacteria



as a function of the  $\text{NaHCO}_3$  concentration in the experimental systems. We observed a strong positive correlation between the measured U(VI) reduction rates and the calculated total concentration of U(VI) surface complexes formed on the bacterial cell envelope. This positive correlation indicates that the speciation and concentration of U(VI) adsorbed on the bacterial cell envelope control the kinetics of U(VI) bioreduction under the experimental conditions. The results of this study serve as a basis for developing speciation-based kinetic rate laws for enzymatic reduction of U(VI) by bacteria.

## INTRODUCTION

A number of groundwater systems have been contaminated by uranium as a result of mining activities or from improper disposal of waste from nuclear materials processing. The mobility of U in the subsurface can be dramatically reduced when soluble U(VI) is reduced to sparingly soluble U(IV) solid phases under anaerobic conditions.<sup>1–3</sup> Enzymatic reduction of U(VI) by bacteria can be both rapid and complete under controlled conditions,<sup>4–6</sup> and hence represents a potentially efficient and inexpensive U remediation approach.<sup>7–9</sup>

In order to understand and model the fate and mobility of U in groundwater systems and also to enhance the effectiveness of U bioremediation strategies, it is crucial to determine the controls on the enzymatic U(VI) bioreduction rate. A considerable amount of research has investigated the mechanisms of U(VI) reduction by bacteria.<sup>10–12</sup> For example, Ulrich et al.<sup>11</sup> examined U(VI) reduction by *Shewanella oneidensis* as a function of dissolved bicarbonate and Ca concentrations, and related the change in reduction kinetics that they observed to changes in the dominant U(VI) species in solution that accompanied changing fluid compositions. Similarly, Stewart et al.<sup>12</sup> observed that dissolved Ca and the presence of iron oxides both decrease the U(VI) reduction rate by affecting the aqueous U(VI) speciation. However, the controls on the kinetics of the reduction process and the connection between aqueous complexation and its effect on

U(VI) reduction rates are still poorly defined, especially in complex realistic geologic systems.

Previous studies suggest that U(VI) speciation and distribution in geologic systems may affect U(VI) reduction rates, but a better understanding of the relationship between U speciation and U bioavailability is needed in order to derive speciation-based kinetic rate laws. Sheng et al.<sup>13</sup> proposed that the speciation of both U(VI) and U(IV) on bacterial cell envelopes controls the kinetics of U(VI) reduction by bacteria. Sheng et al.<sup>13</sup> measured the rate of U(VI) reduction by *S. oneidensis* in the presence of dissolved Ca and EDTA, and found strong correlations between the speciation and concentration of U(VI) on the cell envelope and the U(VI) reduction rate.

Other studies also suggest that metal bioavailability can be linked to the extent and speciation of metal adsorption onto bacterial cell envelopes.<sup>14–16</sup> For example, the chemotactic response of *Escherichia coli* away from aqueous Ni is strongly correlated to the extent of Ni adsorbed onto functional groups on the cell envelope,<sup>15</sup> and the toxicity of U and Cu to bacteria is positively correlated to the concentration of the metals that bind to bacterial cells.<sup>14</sup> In addition, VanEngelen et al.<sup>16</sup>

Received: September 27, 2013

Accepted: February 28, 2014

Published: February 28, 2014

demonstrated that the presence of high concentrations of bicarbonate in solution significantly inhibits the toxicity of U(VI) to bacteria due to the formation of negatively charged uranyl-carbonate aqueous complexes, which are less bioavailable to the bacteria than carbonate-free U(VI) aqueous species. The presence of bicarbonate under circumneutral to basic pH conditions decreases the concentration of U(VI) that adsorbs onto bacteria.<sup>17</sup> Hence, although VanEngelen et al.<sup>16</sup> did not propose a link between adsorption and bioavailability, it is likely that U(VI) bioavailability is controlled by adsorption of U(VI) onto the cell envelope. The decreased toxicity observed by VanEngelen et al.<sup>16</sup> likely was caused by decreased adsorption and/or a change in bacterial cell envelope speciation of U(VI) that accompanied the introduction of bicarbonate to solution.

In order to test the hypothesis that the extent and speciation of U(VI) on the bacterial cell envelope controls the kinetics of enzymatic U(VI) reduction by bacteria, in this study we measured the rate of U(VI) reduction by bacteria as a function of NaHCO<sub>3</sub> concentration in solution. Instead of focusing on the effects of aqueous speciation of U(VI) on U(VI) reduction kinetics, we test whether the observed U(VI) reduction kinetics can be related to the speciation of adsorbed U(VI) on the bacteria in these high carbonate systems. Although Sheng et al.<sup>13</sup> observed a correlation between U(VI) adsorption and enzymatic U(VI) reduction rates, their experiments were conducted only at one concentration of dissolved carbonate, and they only examined the effect of dissolved Ca and EDTA on U(VI) adsorption and U(VI) reduction rates. Bicarbonate not only is ubiquitous in natural geologic systems, but also is commonly used as a flushing agent to mobilize subsurface U in remediation and mining approaches.<sup>18–20</sup> In this study, we probe bioavailability of U(VI) under a range of more elevated bicarbonate concentrations than were studied by Sheng et al.,<sup>13</sup> and thereby we determine the bioavailability of adsorbed uranyl-carbonate complexes. We use stability constants for the important uranyl-bacterial surface complexes to calculate the concentration and speciation of U(VI) on the bacterial cell envelope under each of the experimental conditions, and we test if a relationship exists between the calculated extent of U(VI) adsorption onto the bacterial cell envelope and the observed U(VI) reduction rate. In this study, we test the hypothesis that the reduction rate, and hence the bioavailability of U(VI), is controlled by the concentration of adsorbed U(VI) independent of the aqueous speciation of U(VI) in solution. Determining if such a relationship exists provides insights into the controls on U(VI) bioavailability to bacteria, and is crucial in order to design effective bioremediation strategies based on enzymatic reduction of U(VI) in realistic geologic systems.

## MATERIALS AND METHODS

**Bacteria Preparation.** The facultative Gram-negative bacterium *Shewanella oneidensis* strain MR-1 was used in this study. Cells of *S. oneidensis* were cultured aerobically and prepared following similar procedures to those described previously.<sup>13</sup> Cells were collected by centrifugation at 10 970g for 5 min after 48 h aerobic growth. Cells were washed twice by resuspending them in 20 mL of sterile anoxic NaHCO<sub>3</sub> solution, and then were resuspended in 10 mL of the same solution to make a parent bacterial suspension. The concentration of NaHCO<sub>3</sub> used in the wash solution was the same as the concentration of NaHCO<sub>3</sub> that was to be used in the specific U(VI) reduction experiments for which each batch of bacteria was being prepared. A small portion of the parent

bacterial suspension was sampled in order to measure the actual cell concentration in the suspension following procedures described previously.<sup>21</sup> The rest of the parent bacterial suspension was transferred into an anaerobic glovebox for use in the U(VI) reduction experiments. All the growth media and solutions used in this study were made with ultrapure 18 MΩ water.

**U(VI) Reduction Experiments.** The reduction experiments were conducted inside an anaerobic glovebox chamber with an atmosphere of 95% N<sub>2</sub>/5% H<sub>2</sub>, and with a palladium catalyst heater unit to remove any remnant oxygen. We used a gas analyzer within the glovebox to monitor oxygen concentrations, ensuring that oxygen was present below the 1 ppm detection limit of the analyzer at all times. The general procedures and analytical methods used were similar to those described by Sheng et al.<sup>13</sup> The experimental medium consisted of 50 mM Na-lactate, and NaHCO<sub>3</sub> at either 2.4, 5.0, 7.2, 11.9, 21.0, or 30.0 mM. First, a 50 mM Na-lactate solution was bubbled with a 95% N<sub>2</sub>/5% H<sub>2</sub> gas mixture for ~30 min outside the glovebox to remove dissolved oxygen. The Na-lactate solution was then transferred into the glovebox and separated into serum bottles, which were sealed, removed from the glovebox, and then autoclaved at 120 °C for 20 min. Inside the glovebox, a weighed mass of solid NaHCO<sub>3</sub> was added to a weighed amount of the anoxic sterile 50 mM Na-lactate solution to achieve a NaHCO<sub>3</sub> concentration of 2.4, 5.0, 7.2, 11.9, 21.0, or 30.0 mM. The pH of this lactate-bicarbonate solution was adjusted to be approximately 7.0 using small aliquots of concentrated NaOH and/or HCl. A filter-sterilized (using 0.2 μm nylon membrane filters) uranyl acetate stock solution was prepared as described previously,<sup>13</sup> the concentration of which was determined to be approximately 200 mM by inductively coupled plasma optical emission spectroscopy (ICP-OES). A volume of the uranyl acetate stock solution was added to a weighed volume of the lactate-bicarbonate solution inside a Teflon bottle to achieve an initial aqueous U(VI) concentration of either 0.25 or 0.1 mM. The exact total dissolved U concentration of a sample of this solution was determined by ICP-OES, and was taken to be the initial U(VI) concentration in the reduction experiments. A weighed volume of the parent bacterial suspension was added to a weighed volume of the U(VI)-lactate-bicarbonate solution to achieve an experimental cell concentration of 1.0 g(wet mass) bacteria/L. The wet mass is approximately 8 times the dry mass of the biomass<sup>22</sup> and 1 g wet mass equals approximately  $1.9(\pm 0.6) \times 10^{10}$  cells.<sup>13</sup> After addition of the cells, the experimental suspension was stirred continuously and sampled at selected times. The pH was periodically measured and maintained to be approximately 7.0 by using small aliquots of concentrated NaOH and/or HCl.

U(VI) can adsorb to a significant extent onto *S. oneidensis* at pH 7.0 even in the presence of NaHCO<sub>3</sub>,<sup>17</sup> so it is likely that a portion of the U(VI) that was removed from solution was present as adsorbed U(VI) on the bacterial cells. If we directly measured the U(VI) left in solution only, we would overestimate the reduction rate by failing to account for the U(VI) that was adsorbed onto the bacterial cells. Therefore, in order to measure all of the U(VI) remaining in the system at each sampling time, we conducted an acidification step on each sample that promoted desorption of U(VI) from the bacteria and caused all remaining U(VI) in the system to be present in solution and available for analysis. When sampling, 8 mL was extracted from the reaction vessel and transferred into a Teflon tube, sealed inside the glovebox, and then centrifuged at 6600g

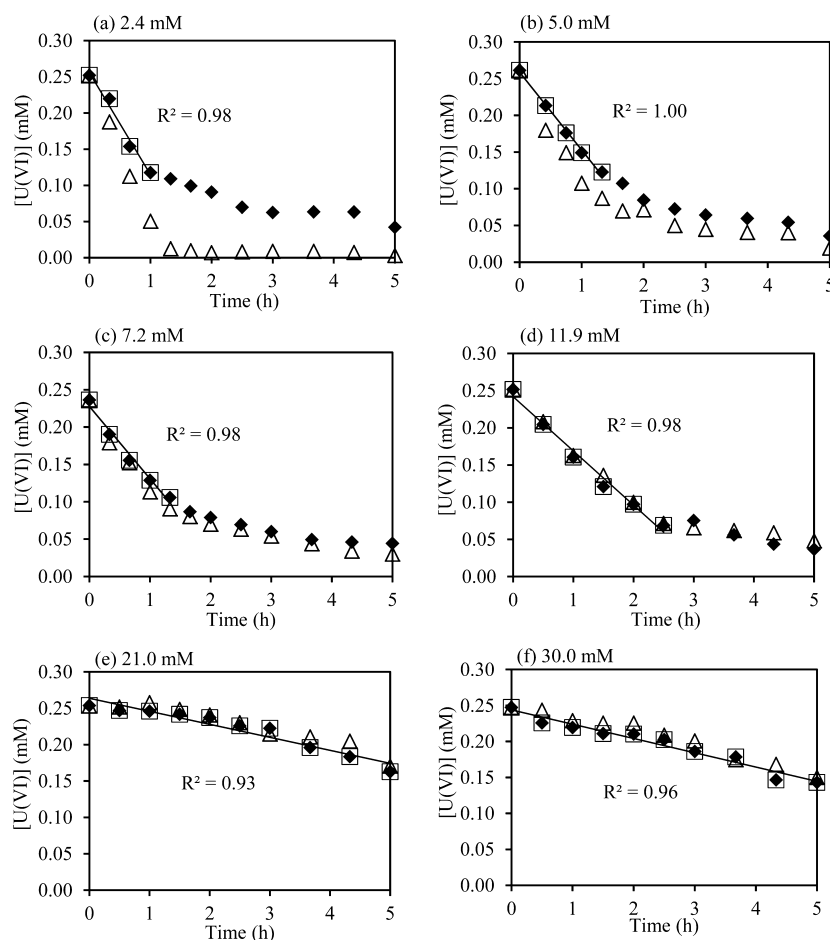


**Figure 1.** The concentrations of dissolved U(VI) remaining in solution in the presence of (a) 2.4 mM; (b) 5.0 mM; (c) 7.2 mM; (d) 11.9 mM; (e) 21.0 mM; (f) 30.0 mM NaHCO<sub>3</sub> as a function of time with an initial U(VI) concentration of 0.25 mM. In each figure, open triangles represent the “before desorption” data set in which the sample was immediately analyzed for concentration of remaining U(VI) at each sampling time; solid diamonds represent the “after desorption” data set in which the sample was acidified to approximately pH 1.5 for ~40 min before analysis of U(VI) concentration; open squares represent the data points used to calculate the initial rate of U(VI) reduction by *S. oneidensis*. The figure depicts one of three replicate experiments conducted under each experimental condition; the remaining two replicates are shown in SI.

for 2 min and filtered through a 0.2  $\mu\text{m}$  Millipore Millex PTFE filter outside the glovebox. The sample was analyzed immediately for dissolved U(VI) concentration by fluorescence spectrometry. Analysis of those samples yields a “before desorption” concentration of U(VI) in the experiment. At each sampling time, a second 8 mL sample was also extracted and transferred to another Teflon tube and acidified with 60  $\mu\text{L}$  of 12.1 N HCl, to decrease the pH of the sample to approximately 1.5. After 40 min of agitation, the acidified sample was sealed inside the glovebox and then transferred to the outside for centrifugation, filtration, and immediate analysis for dissolved U(VI) concentration. Because the acidification step caused all remaining U(VI) in the experimental systems to partition into solution, we used these “after desorption” U(VI) concentrations to define the U(VI) reduction rate. It is possible that the acidification step may cause the desorption of U(IV) and cell lysis; however, the presence of the U(IV) in solution would not affect the subsequent U(VI) analysis. The fact that the U(VI) concentrations in the acidified and nonacidified samples under most studied conditions were nearly identical (see Results below) is strong evidence that the acidification step did not cause any significant reoxidation of U(IV). The reduction experiments were conducted in triplicate for each NaHCO<sub>3</sub> concentration. The experiments with 0.1 mM U(VI)

were only conducted at NaHCO<sub>3</sub> concentrations of 2.4 and 7.2 mM, and in these experiments we only measured the U(VI) concentrations after the acidification step. Previous measurements indicated that the concentrations of dissolved carbonate at pH 7 did not change significantly in 3 h.<sup>17</sup> Because the reduction rate was determined from the data collected in the first 3 h in most of the experiments in this study, it is safe to assume that no significant change in dissolved carbonate concentration occurred in the experiments.

A set of control experiments was carried out under conditions open to the atmosphere to determine if the acidification step in the reduction experiments releases all of the adsorbed U(VI) into solution. Due to the presence of oxygen in the control experiments, no U(VI) reduction occurred and U(VI) adsorption was isolated. In the control experiments, 1.0 g(wet mass)/L of cells prepared as described above was added to a solution which consisted of 50 mM Na-lactate, different concentrations of NaHCO<sub>3</sub> (2.4, 5.0, 7.2, 11.9, 21.0, or 30.0 mM), and 0.25 mM total U (added as uranyl acetate). The pH was maintained at approximately 7.0 for ~2.5 h. The sample was then acidified with 12N HCl to approximately pH 1.5 for 40 min. The cells were removed by centrifugation and filtration, and the concentrations of initial (before addition of cells) and final (after removal of cells) total

dissolved uranium in the solution were determined by ICP-OES. The results of these desorption control experiments indicate that the acidification step promoted desorption of approximately 92% of the total U in the system, and only 8% of the uranium was present as adsorbed U on the cells at pH 1.5. Another set of control experiments with 0.1 mM total U and concentration of 2.4 or 7.2 mM NaHCO<sub>3</sub> were also conducted following the same procedures described above. The results indicate that approximately 75% of the total U was recovered during the acidification step and approximately 25% of the total U remained adsorbed onto cells even at pH 1.5. Cell-free control experiments, which followed the same experimental procedures as the reduction experiments but without the addition of cells, were also conducted in order to determine if any U(VI) was lost due to adsorption onto the experimental apparatus or for any possible reason other than reduction by bacteria. No measurable loss of U(VI) was observed in these abiotic controls.

A PTI Quantamaster QM-4 spectrofluorometer was used to measure the phosphorescence decay of U(VI) in order to determine the concentration of U(VI) in solution, following the general approach and principles described in previous studies.<sup>2,23</sup> Those previous studies used a kinetic phosphorescence analyzer (KPA) which uses a pulsed nitrogen laser as an excitation source and has an extremely low detection limit (~1 ng/L).<sup>23</sup> Similar to KPA, the spectrofluorometer measures phosphorescence decay by recording the change in intensity of the phosphorescence signal emitted by excited U(VI) atoms in the sample as a function of time. The spectrofluorometer that was used in this study uses a xenon flash lamp, and has a higher detection limit (~2 ppm) than KPA. However, because the initial concentration of U(VI) in our experiments was 0.25 mM (~60 ppm), the spectrofluorometer provides adequate U(VI) analytical resolution and precision under our experimental conditions. The setup parameters of the spectrofluorometer and sample preparation were similar to those reported by Sheng et al.<sup>13</sup> Each sample (0.5 mL) was acidified with 0.25 mL of 12.1 N HCl, and diluted 150 times with ultrapure 18 MΩ water. 1.5 mL of Uraplex (complexing agent) was then added to 1 mL of diluted sample and the solution was analyzed immediately on the spectrofluorometer, using an excitation wavelength of 420 nm, an emission wavelength of 515 nm and slit width of 17 nm. Matrix-matched blanks and standards covering the probable range of U(VI) in solution were measured to construct a calibration curve and to quantify the U(VI) concentrations in the samples. Any potential chloride interference was accounted for by maintaining constant chloride concentrations in the standards and the samples. The spectrofluorometer exhibits a linear dynamic range for aqueous U(VI) concentrations from 2 ppm to 90 ppm under our experimental conditions. Analytical uncertainty was approximately ±4.5%, as determined by repeat analyses of an aqueous U(VI) standard.

## RESULTS AND DISCUSSION

**U(VI) Reduction Experiments.** For the reduction experiments with 0.25 mM initial U(VI), acidified samples from experiments with 2.4 and 5.0 mM NaHCO<sub>3</sub> (Figure 1a and b) yielded higher measured U(VI) concentrations than did the nonacidified samples, due to significant adsorption of U(VI) species onto the bacterial cell envelope. However, experiments with higher NaHCO<sub>3</sub> concentrations, depicted in Figure 1c–f, showed no significant difference between the acidified and

nonacidified samples, likely because only a small fraction of the U(VI) adsorbs onto bacterial cell envelope sites at neutral pH in the presence of these higher NaHCO<sub>3</sub> concentrations.<sup>17</sup> Each of the experimental systems exhibited an initial linear decrease in U(VI) concentration as a function of time. For the systems with lower NaHCO<sub>3</sub> concentrations, the observed reduction rate decreased markedly when approximately 60–70% of the original U(VI) had been reduced. The experiments with 21.0 and 30.0 mM NaHCO<sub>3</sub> did not exhibit this change in reduction rate. However, the reduction rates that were observed in these experiments were slower than those observed in the experiments with lower NaHCO<sub>3</sub> concentrations. At the end of the 21.0 and 30.0 mM NaHCO<sub>3</sub> experiments, the U(VI) concentration had only decreased by approximately 30–40% from its original value, so perhaps did not reach a low enough U(VI) concentration to cause the change in reduction rate. In our exercise of relating reduction rates to the speciation and concentration of U(VI) on the bacteria, we only considered the data that define the initial linear reduction rates, with these initial reduction rates depicted in Figure 1 as solid lines. The initial reduction rate for each NaHCO<sub>3</sub> concentration was determined from a linear fit to the U(VI) measurements from the acidified samples only, and was calculated using the data points that defined the initial linear relationship. For example, the initial rate of reduction for the 2.4 mM NaHCO<sub>3</sub> experiment shown in Figure 1a was determined from the first four data points collected during the first 1 h of the experiment, while the reduction rate for the 30.0 mM NaHCO<sub>3</sub> experiment (Figure 1f) was determined from the entire data set.

For the 0.1 mM U(VI) experiments, approximately 0.025 mM U(VI) remained adsorbed onto the cells even after the acidification step according to the results of our desorption control experiment. Using our experimental approach, we cannot determine to what extent the U that remains adsorbed onto the cells after acidification is U(VI). In order to conservatively estimate U(VI) reduction rates, we assume that none of this U(VI) is reduced to U(IV), yielding minimum U(VI) reduction rates under each condition. Hence, 0.025 mM U(VI) was added to the measured U(VI) concentration in solution to obtain the total U(VI) concentration in each sample, and this calculated value was used to determine the U(VI) reduction rates (Figure 2). This correction was not needed for the 0.25 mM U(VI) experiments shown in Figure 1 because 92% of the U(VI) was recovered in the acidification test. The data shown in Figures 1 and 2 are representative ones for each NaHCO<sub>3</sub> concentration. The figures show only one of the three replicate runs. The results for the other two replicates for each NaHCO<sub>3</sub> concentration are included in the Supporting Information (SI). The average initial reduction rate and the associated uncertainty (1σ) for each of these experimental conditions are shown in Table 1, and were calculated from the three experiments conducted at each NaHCO<sub>3</sub> concentration.

The reduction rate data clearly indicate that increasing the concentration of NaHCO<sub>3</sub> in solution significantly decreases the rate of U(VI) reduction by *S. oneidensis* (Figure 3). This observation is consistent with the results of previous studies,<sup>11,24</sup> which note a similar dependence of the U(VI) reduction rate on NaHCO<sub>3</sub> concentration in solution. As the concentration of NaHCO<sub>3</sub> increases from 2.4 to 30.0 mM in the reduction experiments with 0.25 mM initial U(VI), the initial U(VI) reduction rate decreases from 1.256 to 0.216 μmol U(VI)/mg dry biomass/h. The reduction rate also decreases from 0.757 to 0.371 μmol U(VI)/mg dry biomass/h, when

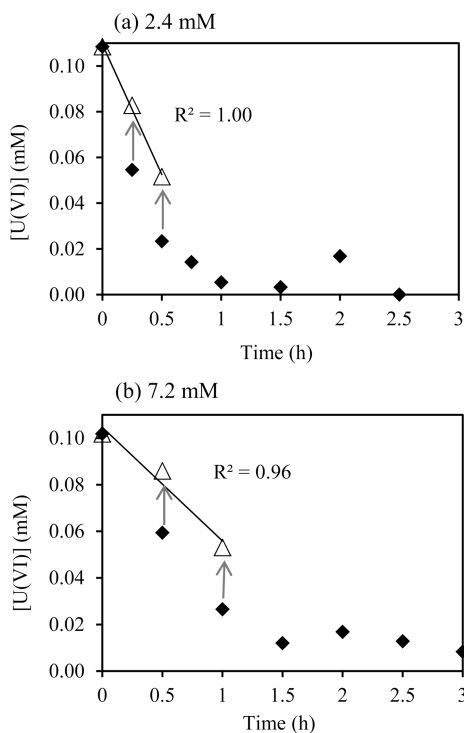


**Figure 2.** The concentrations of U(VI) in the presence of (a) 2.4 mM and (b) 7.2 mM NaHCO<sub>3</sub> as a function of time with an initial U(VI) concentration of 0.1 mM. In each figure, solid diamonds represent the concentrations of dissolved U(VI) remaining in solution after the acidification step; open triangles represent the concentrations of total U(VI) in the system and these were used to calculate the initial reduction rate (see text). The figure depicts one of three replicate experiments conducted under each experimental condition; the remaining two replicates are shown in SI.

**Table 1. Calculated Uranyl Surface Complexes and Average Reduction Rate**

initial U(VI) (mM)	NaHCO <sub>3</sub> (mM)	R-L <sub>2</sub> -(UO <sub>2</sub> ) <sub>2</sub> CO <sub>3</sub> (OH) <sub>3</sub> <sup>2-α</sup> (mM)	total adsorbed U(VI) <sup>b</sup> (mM)	average initial reduction rate [μmol U(VI)/mg dry biomass/h] ± 1σ
0.25	2.4	0.0726	0.1453	1.256 ± 0.112
0.25	5.0	0.0478	0.0956	0.832 ± 0.016
0.25	7.2	0.0259	0.0517	0.736 ± 0.076
0.25	11.9	0.0174	0.0347	0.581 ± 0.028
0.25	21.0	0.0013	0.0026	0.173 ± 0.038
0.25	30.0	0.0002	0.0003	0.216 ± 0.049
0.1	2.4	0.0308	0.0616	0.757 ± 0.136
0.1	7.2	0.0156	0.0312	0.371 ± 0.018

<sup>a</sup>R-L#- represents *S. oneidensis* functional groups, Sites 1- 4, with pK<sub>a</sub> values of 3.3 ± 0.2, 4.8 ± 0.2, 6.7 ± 0.4, and 9.4 ± 0.5, respectively.<sup>30</sup>

<sup>b</sup>Total adsorbed U(VI) includes all the uranyl surface complexes formed on the cell envelope: R-L<sub>1</sub>-UO<sub>2</sub><sup>2+</sup>, R-L<sub>2</sub>-(UO<sub>2</sub>)<sub>3</sub>(OH)<sub>3</sub><sup>0</sup>, R-L<sub>2</sub>-(UO<sub>2</sub>)<sub>4</sub>(OH)<sub>7</sub><sup>0</sup>, R-L<sub>3</sub>-(UO<sub>2</sub>)<sub>3</sub>(OH)<sub>7</sub><sup>2-</sup>, R-L<sub>2</sub>-(UO<sub>2</sub>)<sub>2</sub>CO<sub>3</sub>(OH)<sub>3</sub><sup>2-</sup>.<sup>17</sup>

NaHCO<sub>3</sub> concentration increases from 2.4 mM to 7.2 mM in the reduction experiments with 0.1 mM initial U(VI). In addition, for reduction experiments with the same NaHCO<sub>3</sub> concentration but different initial U(VI) concentration, U(VI) reduction rates decrease with decreasing initial U(VI) concentration, which is consistent with the results from Haas and Northup.<sup>25</sup> The reduction rates that we observed in the 21.0 and 30.0 mM NaHCO<sub>3</sub> experiments with 0.25 mM initial

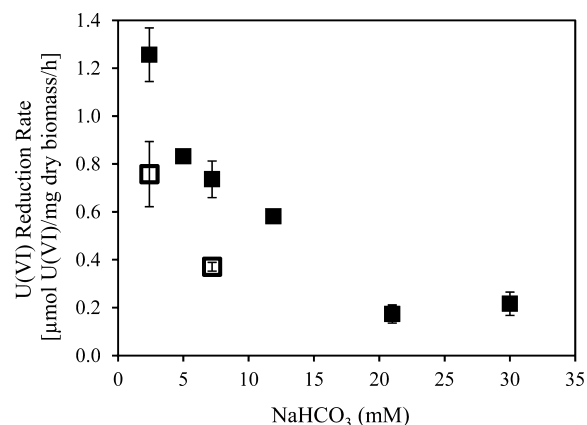


**Figure 3.** The average initial rate of U(VI) reduction by *S. oneidensis* as a function of NaHCO<sub>3</sub> concentration in the experiments. The error bars represent the associated standard deviation (1σ) of each value. Solid and open squares represent data for experiments with initial U(VI) concentrations of 0.25 mM and 0.1 mM, respectively.

U(VI) are the same within experimental uncertainty, with a value of  $0.173 \pm 0.038 \mu\text{mol U(VI)/mg dry biomass/h}$  for the 21.0 mM NaHCO<sub>3</sub> system and a value of  $0.216 \pm 0.049 \mu\text{mol U(VI)/mg dry biomass/h}$  for the 30.0 mM NaHCO<sub>3</sub> system. The lack of an observed effect of increasing NaHCO<sub>3</sub> concentration on the reduction rate under the two highest NaHCO<sub>3</sub> conditions is likely due to the increased difficulty in obtaining precise rate determinations for these conditions where the U(VI) reduction rates are so slow.

**Thermodynamic Modeling.** A nonelectrostatic surface complexation modeling approach and the program FITEQL were used to calculate the extent and speciation of U(VI) that was adsorbed onto the cell envelope of *S. oneidensis* under the initial conditions of the U(VI) reduction experiments.<sup>17,21,26</sup> The extent of adsorption of U(VI) likely changes as a function of time during the experiments, and the observed U(VI) reduction rate also changed with time to some extent (Figure 1). Our objective was to determine merely if the initial reduction rate could be related to the initial extent of U(VI) adsorption. The calculations accounted for aqueous U(VI) complexation with hydroxide and carbonate, and also the important uranyl surface complexation reactions determined by Sheng and Fein<sup>17</sup> for *S. oneidensis* (refer to Table S1 and Table S2 in SI for the reactions considered in the calculations along with corresponding equilibrium constant values and their sources). Although aqueous uranyl hydroxide and carbonate complexation limit the extent of U(VI) adsorption that occurs above pH 5, significant adsorption still occurs even in systems with high dissolved carbonate, and we model U(VI) adsorption in our pH ~ 7 systems using an adsorption reaction between the aqueous complex (UO<sub>2</sub>)<sub>2</sub>CO<sub>3</sub>(OH)<sub>3</sub><sup>-</sup> and a deprotonated bacterial site.<sup>17</sup> Sheng and Fein<sup>17</sup> provide evidence for the adsorption of a negatively charged U(VI) species onto bacteria above pH 5, based on the observation of U(VI) adsorption under conditions where the U(VI) speciation is dominated by (UO<sub>2</sub>)<sub>2</sub>CO<sub>3</sub>(OH)<sub>3</sub><sup>-</sup> and other negatively charged complexes. Despite electrostatic repulsion between (UO<sub>2</sub>)<sub>2</sub>CO<sub>3</sub>(OH)<sub>3</sub><sup>-</sup> and the negatively charged binding site, adsorption can still occur due to favorable energetics of covalent bonding.<sup>27</sup> The speciation calculations indicate that the dominant uranyl-bacterial complex that forms at pH 7.0 under our experimental conditions is R-L<sub>2</sub>-(UO<sub>2</sub>)<sub>2</sub>CO<sub>3</sub>(OH)<sub>3</sub><sup>2-</sup> (Table 1). The extent

of total adsorbed U(VI) at pH 7.0 decreases as the concentration of  $\text{NaHCO}_3$  increases in the experiments with the same initial U(VI) concentration, and the total adsorbed U(V) also decreases with decreasing initial U(VI) concentration in the system (Figure 4).

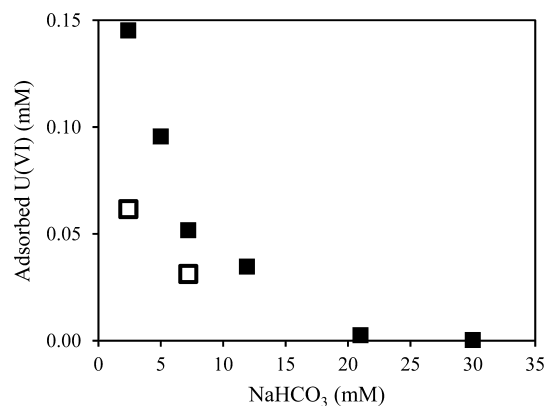


**Figure 4.** The total concentration of U(VI) adsorbed onto the cell envelope of *S. oneidensis* as a function of  $\text{NaHCO}_3$  concentration in the experiments. Solid and open squares represent data for experiments with initial U(VI) concentrations of 0.25 mM and 0.1 mM, respectively.

A strong positive correlation exists between the observed U(VI) reduction rate and the calculated total concentration of U(VI) that adsorbed onto the bacterial cell envelope (Figure 5). It is interesting to note that although the 0.1 mM and the

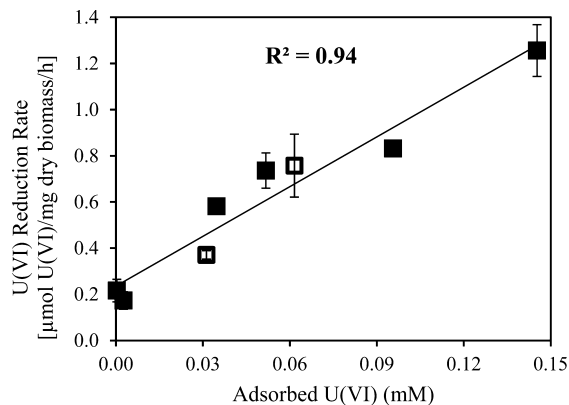


**Figure 5.** Average initial U(VI) reduction rates as a function of the total concentration of U(VI) adsorbed onto the cell envelope of *S. oneidensis*. The error bars represent the associated standard deviation ( $1\sigma$ ) of each value. Solid and open squares represent data for experiments with initial U(VI) concentrations of 0.25 mM and 0.1 mM, respectively.

0.25 mM U(VI) experiments exhibit distinct trends in the relationships between the reduction rate and  $\text{NaHCO}_3$  concentration and between extent adsorbed and  $\text{NaHCO}_3$  concentration (Figures 3 and 4), they define a single trend when the data are translated into reduction rate as a function of extent of adsorption (Figure 5). This result strongly supports our hypothesis that the reduction rate, and hence the bioavailability of U(VI), is controlled by the concentration of adsorbed U(VI) independent of the speciation of U(VI) in solution. Increasing the concentration of  $\text{NaHCO}_3$  in the experimental systems causes a decrease in the extent of U(VI)

adsorption onto the cells, and hence a concomitant decrease in the U(VI) reduction rate by the bacteria. Similarly, decreasing the total U(VI) concentration in the system also causes a decrease in the concentration of adsorbed U(VI) on the bacteria, and hence a decrease in U(VI) reduction rate. These results are consistent with those of Sheng et al.<sup>13</sup> who measured the effect of dissolved Ca on the reduction rate of U(VI) by *S. oneidensis*, and found a strong negative correlation between the reduction rate and the concentration of Ca-uranyl-bacterial complexes, but a strong positive correlation between the U(VI) reduction rate and the total concentration of Ca-free uranyl-bacterial complexes. Our results also suggest a cell envelope speciation control on adsorption. The data from the 2.4, 5.0, and 7.2 mM experiments (Figure 1a–c) indicate that some U(VI) remains adsorbed onto the bacterial cells. At the end of the experiments, the reduction rates are much slower than at the beginning, suggesting that the adsorbed U(VI) at the end of the experiments is not as readily reduced as is the U(VI) that reduces rapidly at the beginning of the experiments. This effect may be caused by the presence of a distinct uranyl-bacteria complex that is not as bioavailable as the dominant form of adsorbed U(VI) at the beginning of the experiments.

Previous studies have suggested that U speciation in solution affects the rate of U(VI) reduction by bacteria.<sup>11,12</sup> However, under the experimental conditions, direct contact between U(VI) and the enzymatic electron pathways within the bacterial cell envelope, specifically multiple sites located in the outer membrane and periplasm,<sup>28,29</sup> is required in order for U(VI) reduction to occur. Therefore, although the extent of adsorption and hence reduction rates are clearly related to aqueous U(VI) speciation, this relationship is indirect only. Our approach of relating the reduction rate to the speciation and concentration of U(VI) on the cell envelope represents a more mechanistic model that reflects the fact that U(VI) adsorption is a necessary step during U(VI) reduction. The results of this study provide the framework for using a surface complexation modeling approach for deriving quantitative rate laws for U(VI) reduction by bacteria. This approach not only provides a more mechanistic model of the adsorption reactions that are responsible for U(VI) reduction than does a traditional biotic ligand model approach, but it also enables flexible predictions of the initial rate of U(VI) reduction by bacteria in complex geologic settings through calculation of the speciation and concentration of U(VI) that adsorbs onto the cell envelope.

The observed rate of U(VI) reduction by *S. oneidensis* in this study decreases with increasing  $\text{NaHCO}_3$  concentration in systems with the same initial U(VI) concentration. We calculated the species and concentration of U(VI) that is adsorbed onto the bacteria under the experimental conditions using the thermodynamic surface complexation model and stability constants for the important uranyl-bacterial complexes developed by Sheng and Fein.<sup>17</sup> There is a strong positive correlation between the calculated concentration of adsorbed U on the bacterial cell envelope and the observed U(VI) reduction rate. The correlation between the U(VI) reduction rate and the total concentration of uranyl surface complexes indicates that the speciation and concentration of U(VI) on the bacterial cell envelope control the kinetics of enzymatic reduction of U(VI) by bacteria, and the modeling approach outlined here represents a means for predicting enzymatic U(VI) reduction kinetics in complex geologic settings. Conditions at a field site can vary significantly in terms of pH, carbonate concentration, competing cation concentrations,

etc. The modeling approach described here enables estimations of the effect of changing conditions on U(VI) reduction rates by calculating how these parameters affect the concentration of adsorbed U(VI). Although we did not relate the observed reduction rate to the concentration of specific bacterial surface complexes, the surface complexation approach enables these types of correlations to be incorporated into kinetic rate laws once calibrated by an appropriate set of measurements. In a broader sense, our results are consistent with a growing body of evidence that suggests that adsorption controls a wide range of bacterial metabolic functions that involve metal cations, and that surface complexation modeling represents a potent approach for quantitatively modeling those processes in complex multicomponent systems.

## ■ ASSOCIATED CONTENT

### Supporting Information

Results of the reduction experiments other than those shown in Figure 1 and Figure 2; and aqueous and surface complexation reactions used in the thermodynamic modeling.<sup>17,30–33</sup> This material is available free of charge via the Internet at <http://pubs.acs.org>.

## ■ AUTHOR INFORMATION

### Corresponding Author

\*Phone: (574) 631-2962; fax: (574) 631-9236; e-mail: [lingshengnd@gmail.com](mailto:lingshengnd@gmail.com).

### Notes

The authors declare no competing financial interest.

## ■ ACKNOWLEDGMENTS

This research was supported by a Bayer Predoctoral Fellowship to L.S., administered through the Center for Environmental Science and Technology (CEST) at University of Notre Dame, and a University of Notre Dame Sustainable Energy Initiative grant to J.F. Dissolved U and U(VI) analyses were conducted using equipment in CEST. We thank Jennifer Szymanowski for technical help with the analyses and experimental setup, and we thank two anonymous journal reviewers whose comments and suggestions significantly improved the presentation of this work.

## ■ REFERENCES

- (1) Langmuir, D. Uranium solution-mineral equilibria at low temperatures with applications to sedimentary ore deposits. *Geochim. Cosmochim. Acta* **1978**, *42* (6), 547–569.
- (2) Gorby, Y. A.; Lovley, D. R. Enzymic uranium precipitation. *Environ. Sci. Technol.* **1992**, *26* (1), 205–207.
- (3) Senko, J. M.; Istok, J. D.; Sufliata, J. M.; Krumholz, L. R. In-situ evidence for uranium immobilization and remobilization. *Environ. Sci. Technol.* **2002**, *36* (7), 1491–1496.
- (4) Lovley, D. R.; Phillips, E. J. P.; Gorby, Y. A.; Landa, E. R. Microbial reduction of uranium. *Nature* **1991**, *350*, 413–416.
- (5) Francis, A. J.; Dodge, C. J.; Lu, F.; Halada, G. P.; Clayton, C. R. XPS and XANES studies of uranium reduction by *Clostridium* sp. *Environ. Sci. Technol.* **1994**, *28* (4), 636–639.
- (6) Sani, R. K.; Peyton, B. M.; Smith, W. A.; Apel, W. A.; Petersen, J. N. Dissimilatory reduction of Cr(VI), Fe(III), and U(VI) by *Cellulomonas* isolates. *Appl. Microbiol. Biotechnol.* **2002**, *60* (1–2), 192–99.
- (7) Phillips, E. J. P.; Landa, E. R.; Lovley, D. R. Remediation of uranium contaminated soils with bicarbonate extraction and microbial U(VI) reduction. *J. Ind. Microbiol.* **1995**, *14* (3–4), 203–207.

- (8) Finneran, K. T.; Anderson, R. T.; Nevin, K. P.; Lovley, D. R. Potential for bioremediation of uranium-contaminated aquifers with microbial U(VI) reduction. *Soil Sediment Contam.* **2002**, *11* (3), 339–357.

- (9) Anderson, R. T.; Vrionis, H. A.; Ortiz-Bernad, I.; Resch, C. T.; Long, P. E.; Dayvault, R.; Karp, K.; Marutzky, S.; Metzler, D. R.; Peacock, A.; White, D. C.; Lowe, M.; Lovley, D. R. Stimulating the in situ activity of *Geobacter* species to remove uranium from the groundwater of a uranium-contaminated aquifer. *Appl. Environ. Microbiol.* **2003**, *69* (10), 5884–5891.

- (10) Brooks, S. C.; Fredrickson, J. K.; Carroll, S. L.; Kennedy, D. W.; Zachara, J. M.; Plymale, A. E.; Kelly, S. D.; Kemner, K. M.; Fendorf, S. Inhibition of bacterial U(VI) reduction by calcium. *Environ. Sci. Technol.* **2003**, *37* (9), 1850–1858.

- (11) Ulrich, K.; Veeramani, H.; Bernier-Latmani, R.; Giammar, D. E. Speciation-dependent kinetics of uranium(VI) bioreduction. *Geomicrobiol. J.* **2011**, *28* (5–6), 396–409.

- (12) Stewart, B. D.; Amos, R. T.; Nico, P. S.; Fendorf, S. Influence of uranyl speciation and iron oxides on uranium biogeochemical redox reactions. *Geomicrobiol. J.* **2011**, *28* (5–6), 444–456.

- (13) Sheng, L.; Szymanowski, J.; Fein, J. B. The effects of uranium speciation on the rate of U(VI) reduction by *Shewanella oneidensis* MR-1. *Geochim. Cosmochim. Acta* **2011**, *75* (12), 3558–3567.

- (14) Franklin, N. M.; Stauber, J. L.; Markich, S. J.; Lim, R. P. pH-dependent toxicity of copper and uranium to a tropical freshwater alga (*Chlorella* sp.). *Aquat. Toxicol.* **2000**, *48* (2–3), 275–289.

- (15) Borrok, D.; Borrok, M. J.; Fein, J. B.; Kiessling, L. L. Link between chemotactic response to Ni<sup>2+</sup> and its adsorption onto the *Escherichia coli* cell surface. *Environ. Sci. Technol.* **2005**, *39* (14), 5227–5233.

- (16) VanEngelen, M. R.; Field, E. K.; Gerlach, R.; Lee, B. D.; Apel, W. A.; Peyton, B. M. UO<sub>2</sub><sup>2+</sup> speciation determines uranium toxicity and bioaccumulation in an environmental *Pseudomonas* sp. isolate. *Environ. Toxicol. Chem.* **2010**, *29* (4), 763–769.

- (17) Sheng, L.; Fein, J. B. Uranium adsorption by *Shewanella oneidensis* MR-1 as a function of dissolved inorganic carbon concentration. *Chem. Geol.* **2013**, *358*, 15–22.

- (18) Zhou, P.; Gu, B. Extraction of oxidized and reduced forms of uranium from contaminated soils: Effects of carbonate concentration and pH. *Environ. Sci. Technol.* **2005**, *39* (12), 4435–4440.

- (19) Santos, E. A.; Ladeira, A. C. Q. Recovery of uranium from mine waste by leaching with carbonate-based reagents. *Environ. Sci. Technol.* **2011**, *45* (8), 3591–3597.

- (20) *Uranium Extraction Technology*, Technical Reports Series No. 359; International Atomic Energy Agency: Vienna, 1993; [http://www-pub.iaea.org/MTCD/publications/PDF/trs359\\_web.pdf](http://www-pub.iaea.org/MTCD/publications/PDF/trs359_web.pdf).

- (21) Fein, J. B.; Boily, J. F.; Yee, N.; Gorman-Lewis, D.; Turner, B. F. Potentiometric titrations of *Bacillus subtilis* cells to low pH and a comparison of modeling approaches. *Geochim. Cosmochim. Acta* **2005**, *69* (5), 1123–1132.

- (22) Borrok, D.; Turner, B. F.; Fein, J. B. A universal surface complexation framework for modeling proton binding onto bacterial surfaces in the geological settings. *Am. J. Sci.* **2005**, *305*, 826–853.

- (23) Brina, R.; Miller, A. G. Direct detection of trace levels of uranium by laser-induced kinetic phosphorimetry. *Anal. Chem.* **1992**, *64* (13), 1413–1418.

- (24) Luo, W.; Wu, W. M.; Yan, T.; Criddle, C. S.; Jardine, P. M.; Zhou, J.; Gu, B. Influence of bicarbonate, sulfate, and electron donors on biological reduction of uranium and microbial community composition. *Appl. Microbiol. Biotechnol.* **2007**, *77* (3), 713–721.

- (25) Haas, J. R.; Northup, A. Effects of aqueous complexation on reductive precipitation of uranium by *Shewanella putrefaciens*. *Geochem. Trans.* **2004**, *5* (3), 41–48.

- (26) Herbelin, A.; Westall, J. C. *FITEQL 3.1, A Computer Program for Determination of Chemical Equilibrium Constants from Experimental Data*, Report 94–01; Department of Chemistry, Oregon State University: Corvallis, OR, 1994.

- (27) Kelly, S. D.; Kemner, K. M.; Fein, J. B.; Fowle, D. A.; Boyanov, M. I.; Bunker, B. A.; Yee, N. X-ray absorption fine structure

determination of pH-dependent U-bacterial cell wall interactions. *Geochim. Cosmochim. Acta* **2002**, *66*, 3855–3871.

(28) Beliaev, A. S.; Saffarini, D. A.; McLaughlin, J. L.; Hunnicutt, D. MtrC, an outer membrane decahaem c cytochrome required for metal reduction in *Shewanella putrefaciens* MR-1. *Mol. Microbiol.* **2001**, *39* (3), 722–730.

(29) Wall, J. D.; Krumholz, L. R. Uranium reduction. *Annu. Rev. Microbiol.* **2006**, *60*, 149–166.

(30) Mishra, B.; Boyanov, M.; Bunker, B. A.; Kelly, S. D.; Kemner, K. M.; Fein, J. B. High- and low-affinity binding sites for Cd on the bacterial cell walls of *Bacillus subtilis* and *Shewanella oneidensis*. *Geochim. Cosmochim. Acta* **2010**, *74* (15), 4219–4233.

(31) Martell, A. E.; Smith, R. M. *Critical Stability Constants*; Plenum Press: New York, 1977.

(32) Guillaumont, R.; Fanghänel, T.; Fuger, J.; Grenthe, I.; Neck, V.; Palmer, D. A.; Rand, M. H. *Update on the Chemical Thermodynamics of Uranium, Neptunium, Plutonium, Americium and Technetium*, OECD Nuclear Energy Agency (Ed.); Elsevier: Amsterdam, 2003.

(33) Martell, A. E.; Smith, R. M. *NIST Critically Selected Stability Constants of Metal Complexes, Database 46, Version 6.0 for Windows*; U.S. Department of Commerce, Technology Administration, National Institute of Standards and Technology: Gaithersburg, MD, 2001.